OPEN

Journal of Cerebral Blood Flow & Metabolism (2013) 33, 1015–1024

www.jcbfm.com

ORIGINAL ARTICLE

The sonic hedgehog pathway mediates brain plasticity and subsequent functional recovery after bone marrow stromal cell treatment of stroke in mice

Xiaoshuang Ding[1,2], Yi Li[2], Zhongwu Liu[2], Jing Zhang[2], Yisheng Cui[2], Xiaoguang Chen[1] and Michael Chopp[2,3]

Bone marrow stromal cells (MSCs) improve neurologic recovery after middle cerebral artery occlusion (MCAo). To examine whether *in vivo* blockage of the endogenous sonic hedgehog (Shh) pathway affects grafted MSC-induced neurologic benefits, MCAo mice were administered: vehicle (control); cyclopamine (CP)— a specific Shh pathway inhibitor; MSC; and MSC and cyclopamine (MSC-CP). Neurologic function was evaluated after MCAo. Electron microscopy and immunofluorescence staining were employed to measure synapse density, protein expression of tissue plasminogen activator (tPA), and Shh in parenchymal cells in the ischemic boundary zone (IBZ), respectively. Marrow stromal cell treatment significantly enhanced functional recovery after ischemia, concurrent with increases of synaptophysin, synapse density, and myelinated axons along the IBZ, and significantly increased tPA and Shh expression in astrocytes and neurons compared with control. After treatment with MSC-CP or CP, the above effects were reversed. Co-culture of MSCs with cortical neurons confirmed the effect of Shh on MSC-mediated neurite outgrowth. Our data support the hypothesis that the Shh pathway mediates brain plasticity via tPA and thereby functional recovery after treatment of stroke with MSCs.

Journal of Cerebral Blood Flow & Metabolism (2013) **33,** 1015–1024; doi:10.1038/jcbfm.2013.50; published online 3 April 2013

Keywords: cyclopamine; marrow stromal cells; MCAo; neurite outgrowth; sonic hedgehog

INTRODUCTION

Bone marrow stromal cell (MSC) therapy facilitates neurite outgrowth and improves recovery of neurologic function after stroke.[1,2] Marrow stromal cell treatment of stroke accelerates axonal sprouting and regeneration, decreases the thickness of the glial scar wall,[1] and enhances intercortical and intracortical axonal connections.[3] Our prior studies demonstrate that MSCs modulate endogenous tissue plasminogen activator (tPA) level and activity in the ischemic boundary zone (IBZ) in mice subjected to middle cerebral artery occlusion (MCAo), and tPA plays a pivotal role in neurite outgrowth possibly via the Shh signaling pathway.[4,5] *In vitro* data support the hypothesis that Shh causes the increase in tPA and thereby promotes neurite outgrowth.[6,7] Whether MSC treatment of stroke produces therapeutic restorative effects via Shh and tPA is unclear.

Sonic hedgehog (Shh), a secreted glycoprotein, is a member of the family of the hedgehog proteins. The Shh signaling pathway is well conserved.[8] Sonic hedgehog binds to the transmembrane receptor protein, Patched, to activate another transmembrane receptor, Smoothened, and induces intracellular reactions that target the Gli family of transcription factors. Cyclopamine is a specific inhibitor of Smoothened and can block the Shh pathway. During morphogenesis, Shh is involved in embryonic development and postnatal repair by regulating cell proliferation, migration, differentiation, cell survival, and axonal guidance.[8] However, to our knowledge, there have been no *in vivo* studies explicitly demonstrating the role of the Shh pathway as mediating cell-based restorative therapeutic effects post stroke.

We, therefore, tested the hypothesis that MSCs stimulate tPA activity via the Shh pathway in parenchymal cells to promote neurite outgrowth and improve neurologic function recovery post stroke. Measurements of Shh and tPA expression in parenchymal cells in the IBZ were performed after treatment of stroke with MSCs. Mice were subjected to MCAo and were treated with MSCs, and the direct role of the Shh pathway in mediating neurologic recovery was evaluated using the specific Shh inhibitor, cyclopamine. The data indicate that MSC treatment stimulated the Shh pathway, which increased tPA expression, and thereby improved neurologic function recovery after stroke.

MATERIALS AND METHODS

Middle Cerebral Artery Occlusion Model

Adult male C57BL/6J mice ($n = 45$, age 8–12 weeks, weight 22–26 g) were obtained from Charles River (Wilmington, MA, USA), and were subjected to permanent right-sided MCAo using a method of intraluminal vascular occlusion modified in our laboratory. Briefly, mice were initially anesthetized with isoflurane in 30% O_2 and 70% N_2O using a facemask. The right common carotid artery, external carotid artery, and internal carotid artery were exposed. A length of 6–0 surgical nylon suture with an expanded tip by heating near a flame, was advanced from the right external carotid artery into the lumen of the internal carotid artery to block the origin of the MCA. All experimental procedures were approved by the Institutional Animal Care and Use Committee of Henry Ford Hospital.

[1]Department of Pharmacology, Institute of Materia Medica, Chinese Academy of Medical Sciences, Peking Union Medical College, Beijing, People's Republic of China; [2]Department of Neurology, Henry Ford Hospital, Detroit, Michigan, USA and [3]Department of Physics, Oakland University, Rochester, Michigan, USA. Correspondence: Dr M Chopp, Department of Neurology, Henry Ford Hospital, 2799 West Grand Boulevard, Detroit, MI 48202, USA.
E-mail: chopp@neuro.hfh.edu
This study was supported by R01 AG037506 (MC), R01 NS66041 (YL).
Received 24 January 2013; revised 5 March 2013; accepted 7 March 2013; published online 3 April 2013

Treatment and Tissue Preparation

To investigate if MSCs can stimulate tPA activity via the Shh pathway in parenchymal cells after stroke, we compared the treatment effects of MSCs and MSCs together with cyclopamine (CP), a specific inhibitor of Shh. As CP was dissolved in 2- hydroxypropyl-β-cyclodextrin (HPβCD) solution,[9,10] mice treated with HPβCD were employed as a vehicle control group. HPβCD has low toxicity, including minor hematological changes and reversible histopathological changes in rats, dogs, and monkeys, but did not show any toxicity in mice after either oral or intravenous administration up to a period of 12 months, and no behavioral or neurologic effects in these species were evident;[11] therefore, additional control groups with MSC alone or phosphate buffer solution (PBS) were not employed in this study. In brief, 24 hours (h) after MCAo, mice were randomly divided into four groups: (1) vehicle (control, $n = 12$), 10 mL/kg 45% HPβCD dissolved with PBS was administered by intraperitoneal injection once a day for 7 continuous days; (2) cyclopamine (CP, $n = 9$), 1 mg/mL CP dissolved in 45% HPβCD was administered in 10 mg/kg by intraperitoneal injection once a day for 7 continuous days; (3) MSC ($n = 12$), 1×10^6 MSCs in 0.5 mL PBS was slowly injected into a tail vein over 5 minutes and 10 mL/kg 45% HPβCD dissolved with PBS was administered by intraperitoneal injection once a day for 7 continuous days. Human MSCs were purchased from Cognate Bioservices (Baltimore, MD, USA). (4) MSC and CP (MSC-CP, $n = 12$), 1×10^6 MSCs in 0.5 mL PBS was slowly injected into a tail vein over 5 minutes and 1 mg/mL CP dissolved in 45% HPβCD was administered in 10 mg/kg by intraperitoneal injection once a day for 7 continuous days.

Mice were euthanized under deep ketamine anesthesia at 14 days after MCAo, and were transcardially perfused with 0.9% saline. To analyze the synapse density, 12 mice ($n = 3$/group) were used for EM. A series of 2 mm $\times$ 2 mm $\times$ 1 mm blocks were obtained from the striatum in the IBZ of the ipsilateral hemisphere and the homologous area of the contralateral hemisphere in the forebrain, corresponding to coronal coordinates for bregma -0.5 to 2.5 mm (antero-posterior), 4–6 mm from the sagittal suture (midline to lateral) and 3–4 mm vertical to the dura . The remaining 33 brains (control, MSC, and MSC-CP, $n = 9$; CP, $n = 6$, respectively) were used for histochemistry staining. A standard frozen block (within the center of the lesion of MCAo), corresponding to coronal coordinates for bregma -0.5–0.5 mm was obtained from which a series of 8 μm thickness was employed for histochemistry and immunostaining.

Neurologic Functional Tests

To evaluate the functional recovery, a Foot-Fault test and a modified neurologic severity score (mNSS) evaluation were performed before the treatment after MCAo (baseline, day 1) and at day 3 and 7 after MCAo, and before killing at day 14 by an investigator who was masked to the experimental group, as previously described.[12] The Foot-Fault test measures the accuracy of forepaw placement on a non-equidistant grid as the percentage of Foot-Fault of the left forepaw to total steps. The mNSS is a composite of motor, sensory, reflex, and balance tests, graded on a scale of $0 - 14$ (normal score 0; maximal deficit score 14) for mice. In the severity scores of injury, one score point is awarded for the inability to perform the test or for the lack of a tested reflex; thus, the higher the score, the more severe is the injury.

Electron Microscopy

The specimens ($n = 3$/group) were collected and cut as 2 mm $\times$ 2 mm $\times$ 1 mm pieces, and fixed in 2.5% phosphate-buffered glutaraldehyde for 24 hours. They were then placed, in turn, into 1% osmium tetroxide, gradients of 25%, 50%, 75%, and 95% ethanol, propylene oxide, and embedded in a 50:50 mixture of propylene oxide:araldite resin and 100% araldite. The blocks were shaken, then evacuated to remove the propylene oxide and oven dried at 60 °C 24 hours. Post thin sectioning, the blocks were stained in uranyl acetate and lead citrate 10 minutes each, and then examined at 70 kV on a Philips EM 208 electron microscope (Philips, Eindhoven, The Netherlands). Images were obtained on an AMT XR50 digital imaging system (Advanced Microscopy Techniques, Woburn, MA, USA).

For the analysis of synapse density, 10 electron micrographs (final magnification 36,000) from five fields in the striatum of ipsilateral and contralateral brain were randomly selected. The numbers of synapses were measured with Image J software (NIH, Bethesda, MD, USA). The synapse density was calculated as the percentage of the synapse number counted in the ischemic ipsilateral hemisphere divided by the number of synapse in the homologous contralateral hemisphere.

Histochemical and Immunohistological Assessment

Bielschowsky and Luxol fast blue histochemistry staining or immunostaining were performed. Double staining for Bielschowsky and Luxol fast blue was used to demonstrate axons and myelin,[13] respectively. Briefly, for Bielschowsky staining, frozen brain slides were placed in 20% silver nitrate in the dark, then ammonium hydroxide was added to stained slides until the tissue turned brown with a gold background, and were then treated with sodium thiosulfate. These slides were further stained in Luxol fast blue solution, washed in 95% alcohol, and then placed in lithium carbonate. Nuclei appear colorless, myelin turquoise, and axons appear black on a pale gray/blue background.

For single staining, sections were incubated with primary antibodies against synaptophysin (1:100, 60 min, RT, Chemicon, Temecula, CA, USA). Then the sections were incubated with corresponding fluorescein isothiocyanate (FITC, Calbiochem, Wilmington, MA, USA)-conjugated or cyanine-3 (Cy3; Jackson Immunoresearch, West Grove, PA, USA)-conjugated secondary antibodies, respectively. For double staining, sections were incubated with the first primary antibodies against tPA (1:50; Santa Cruz Biotech, Santa Cruz, CA, USA) or Shh (1:50; Santa Cruz Biotech) followed by the Cy3 conjugated antibody as the chromogen, and then these sections were then incubated with the second primary antibodies against glial fibrillary acidic protein (GFAP, an astrocyte marker, 1:1000; Santa Cruz Biotech), or NeuN (1:500; Chemicon) followed with the FITC-conjugated antibody as the chromogen. 6-Diamidino-2-phenylindole was employed for nucleus staining. Negative control sections from each animal received identical preparations for immunohistochemical staining, except that the primary antibodies were omitted.

Astrocytes and Marrow Stromal Cells Co-culture

Astrocytes (C8-D1A, ATCC, CRL-2541TM) and MSCs (Cognate Bioservices) were cultured in the upper chamber of the transwell insert dish for 24-well plate (Becton Dickinson Labware, FALCON, Franklin Lakes, NJ, USA) together in high glucose Dulbecco's modified eagle medium (DMEM, Invitrogen, San Diego, CA, USA) with 10% fetal bovine serum. In brief, astrocytes (5×10^3) were first seeded, while being up to 70% confluence, the medium was replaced with nonglucose culture media and the astrocytes were put into an anaerobic chamber (model 1025, Forma Scientific, OH, USA) with oxygen-glucose deprivation (OGD) for 2 hours to mimic the transient ischemic situation, or only placed in normal culture without OGD. Then, MSCs (5×10^2) were seeded together with the normal or OGD astrocytes in a total of 0.4 mL media. To further study if MSC treatment of stroke has an effect on neurite remodeling, we used neurons subjected to OGD as an *in vitro* model of cerebral ischemia. As the astrocyte is the most numerous parenchymal cell, and the interaction of MSCs with ischemic brain parenchymal cells likely mediates the therapeutic benefits of MSCs, we treated normal or OGD neurons with the co-cultured astrocytes and MSCs.

Cortical Neuron Primary Culture

Cortical neurons were harvested from embryonic day 17–18 mice. Cultures were prepared according to a previously described procedure with some modifications.[14] Briefly, the embryonic cerebral cortex was dissociated in Ca^{2+} and Mg^{2+} free Hanks balance salt solution containing 0.125% trypsin digestion for 15 minutes. The cell suspensions were washed and re-suspended with Dulbecco's Modified Eagle Medium (DMEM, Invitrogen) in which 5% fetal bovine serum (FBS, GIBCO, Grand Island, NY, USA) was supplemented. After filtered with cell strainers (BD Falcon REF 352350), the neurons were seeded into 2 poly-L-lysine precoated 24-well plates in a density of 10^4 cells/well, and a total of 30 wells were obtained. Incubated at 37 °C with 5% CO_2 for 24 hours, the medium was replaced with serum-free neurobasal medium (Invitrogen) with 2% B-27 (GIBCO), 0.5 mM L-glutamine, and 1% antibiotic–antimycotic. Three days later, 15 of 30 wells of neurons were subjected to OGD, in which the culture medium was replaced with Hanks balance salt solution, and the cells were placed in an anaerobic chamber continuously perfused with 85%/5%/10% $NO_2/CO_2/H_2$ for 2 h. The other 15 wells of neurons were normal cultured. The normal cultured and OGD neurons were treated with either: (1) neural basal medium as control, (2) neural basal medium with 20 μM CP, (3) neural basal medium with 100 ng/mL Shh, (4) normal cultured astrocytes co-cultured with MSCs in the upper chamber of the transwell insert dish, (5) OGD astrocytes co-cultured with MSCs in the upper chamber of the transwell insert dish.

Neurite Outgrowth Assay

Neurons were fixed with 4% paraformaldehyde after 5 days in culture, and identified with immunofluorescence staining of beta tubulin (Tuj1). To analyze neurite outgrowth, Tuj1-positive cells were digitized using an $\times 20$ objective (Zeiss) via the MicroComputer Imaging Device (MCID) system (Imaging Research, St Catharines, Ontario, Canada). Neurite outgrowth was quantified using a software program developed in our laboratory that includes measurements of the branch number and length. Briefly, first, the area of a neuron was labeled; the branches not belonging to the highlighted neuron were then trimmed; the remaining branches surrounding our highlighted neuron were then identified by the software and analyzed; the results were inserted into an Excel file as total neurite number and length. Fifty Tuj1-positive cells per group were measured.

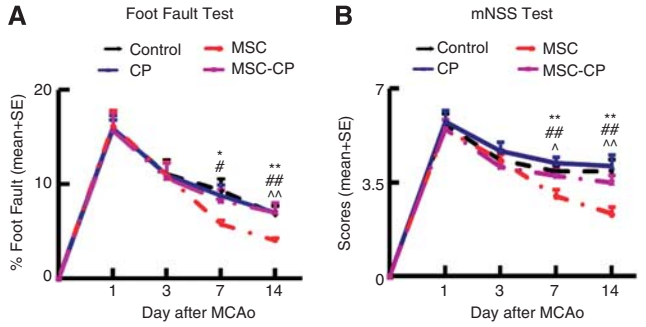

Figure 1. Marrow stromal cell (MSC) treatment significantly promoted functional recovery compared with control at days 7 and 14 ($P<0.05$) post stroke, but this functional benefit was reversed by combination with cyclopamine or cyclopamine mono-treatment. Marrow stromal cell combined with cyclopamine or cyclopamine mono-treatment did not show any functional difference compared with the control mice at any time points. Foot-Fault (**A**); mNSS, modified neurologic severity score (**B**). Control: mice administered with 2-hydroxypropyl-β-cyclodextrin, $n=12$; CP: mice administered with cyclopamine, $n=9$; MSC: mice administered with bone MSCs, $n=12$; MSC-CP: mice administered with bone MSCs and cyclopamine, $n=12$. $^{*}P\leqslant0.05$,$^{**}P\leqslant0.01$ control versus MSC; $^{\#}P\leqslant0.05$, $^{\#\#}P\leqslant0.01$ CP versus MSC; $^{\wedge}P\leqslant0.05$, $^{\wedge\wedge}P\leqslant0.01$ MSC-CP versus MSC.

Enzyme-Linked Immunoabsorbent Assay Detection of Sonic Hedgehog Expression

For the quantitative determination of Shh in the medium from different treated neurons, a mouse Shh N-Terminus Immunoassay ELISA kit (R&D Systems, Minneapolis, MN, USA, Catalog No. MSHH00) was used according to the manufacturer's instructions. Sonic hedgehog was then quantified by colorimetric immunoassay at 450 nm (correction wavelength at 540 nm) by an automated microplate reader according to kit instructions. The absorbance background signal was subtracted from all of the values reported.

Quantification

For measurements of axon density and synaptophysin density, nine fields of view (four from the cortex, four from the striatum and one from the corpus callosum) selected along the IBZ within the ipsilateral hemisphere were digitized and evaluated. The positive area was measured with the MCID software. To measure immunoreactive cells, numbers of $NeuN^{+}$, $GFAP^{+}$, tPA^{+}, and Shh^{+} cells were counted and evaluated using an average number of three histology slides (8 μm thickness, 80 μm interval, every 11 slides) with Image J software, and nine fields of view along the IBZ were digitized under a $\times 40$ objective of a fluorescence microscope.

Statistical Analysis

The functional recovery data were evaluated for normality and ranked data were used for the analysis because the data, especially 'mNSS' were not normally distributed. The global test using Generalized Estimating Equation was implemented to test effects of the treatments on functional recovery at each time point.[15] Significance between different treatments was analyzed with the two tailed Student's *t*-test (for 2 groups) and the analysis of variance (for >2 groups) by using Microsoft Excel 2000 (Microsoft, Redmond, WA, USA) or SPSS 11.5 (SPSS, Chicago, IL, USA). Data are presented as mean ± s.e. A value of $P\leq0.05$ was considered significant.

RESULTS

Neurologic Outcome

The functional recovery after stroke was assessed by the Foot-Fault test and mNSS evaluation (Figures 1A and B). Mice treated with MSCs showed significant functional improvement at

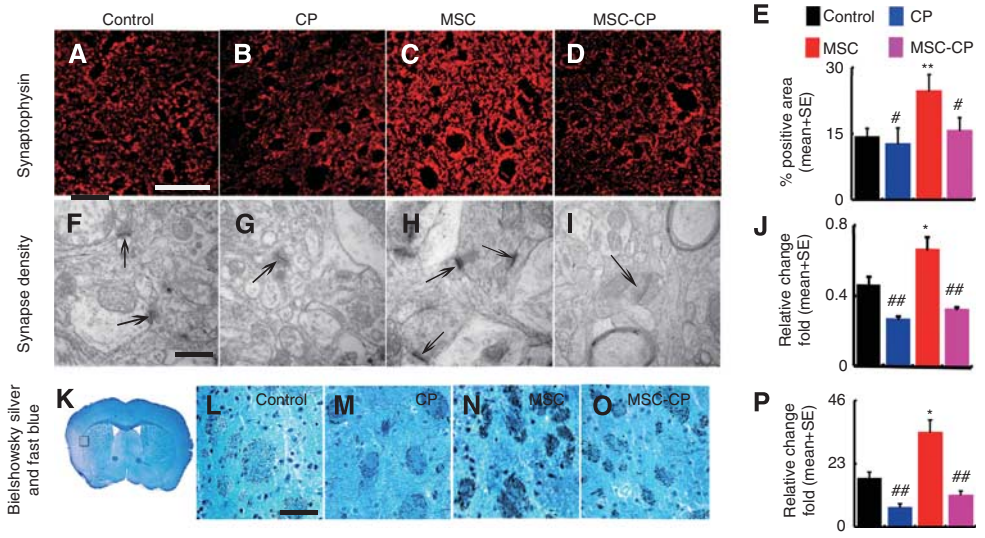

Figure 2. Marrow stromal cell (MSC) treatment increased synaptophysin expression (**A**–**E**, immunohistological staining), synapse density (**F**–**J**, electron microscopy) and axonal remodeling (**K**–**P**, histochemical staining). There was no difference among marrow stromal cells and cyclopamine (MSC-CP), cyclopamine (CP) and control mice. Control: mice administered with 2-hydroxypropyl-β-cyclodextrin; CP: mice administered with cyclopamine; MSC: mice administered with bone MSCs; MSC-CP: mice administered with bone marrow stromal cells and cyclopamine. Synaptophysin and Bielschowsky silver and fast blue: control, MSC and MSC-CP, $n=12$; CP, $n=9$. Synapse density, $n=3$/group, arrows show the synapses. $^{*}P<0.05$, $^{**}P<0.01$ versus Control; $^{\#}P<0.05$, $^{\#\#}P<0.01$ versus MSC. Scale bars: (**A**) = 50 μm; (**F**) = 0.5 μm; (**L**) = 25 μm.

day 7 and 14 post MCAo on the Foot-Fault test (Figure 1A) and mNSS (Figure 1B) evaluation compared with control mice ($P<0.05$, 0.01). To test if the MSC treatment enhancement of functional recovery is mediated by the Shh pathway, we treated mice with CP combined with MSCs or CP alone. At days 7 and 14 post stroke, all mice treated by these two methods showed significantly reduced functional scores compared with MSC treated mice ($P<0.05$), but did not show any functional difference compared with control mice at any time points. These data suggest that the therapeutic effect of MSCs is mediated by the Shh pathway.

Synaptic Plasticity and Neurite Remodeling in the Ischemic Boundary Zone

Synaptic reorganization is important for neurologic functional improvement after stroke;[16] therefore, synaptophysin expression and synaptic density were used to evaluate synaptic plasticity and synaptogenesis.[17] Immunostaining showed that MSC treatment significantly increased synaptophysin expression in the striatum of the IBZ compared with the other treatments described above ($P<0.05$, Figures 2A–E). Additionally, using electron microscopy, we measured the synaptic density in the striatum of the IBZ and the contralateral homologous area (Figures 2F–I). We calculated

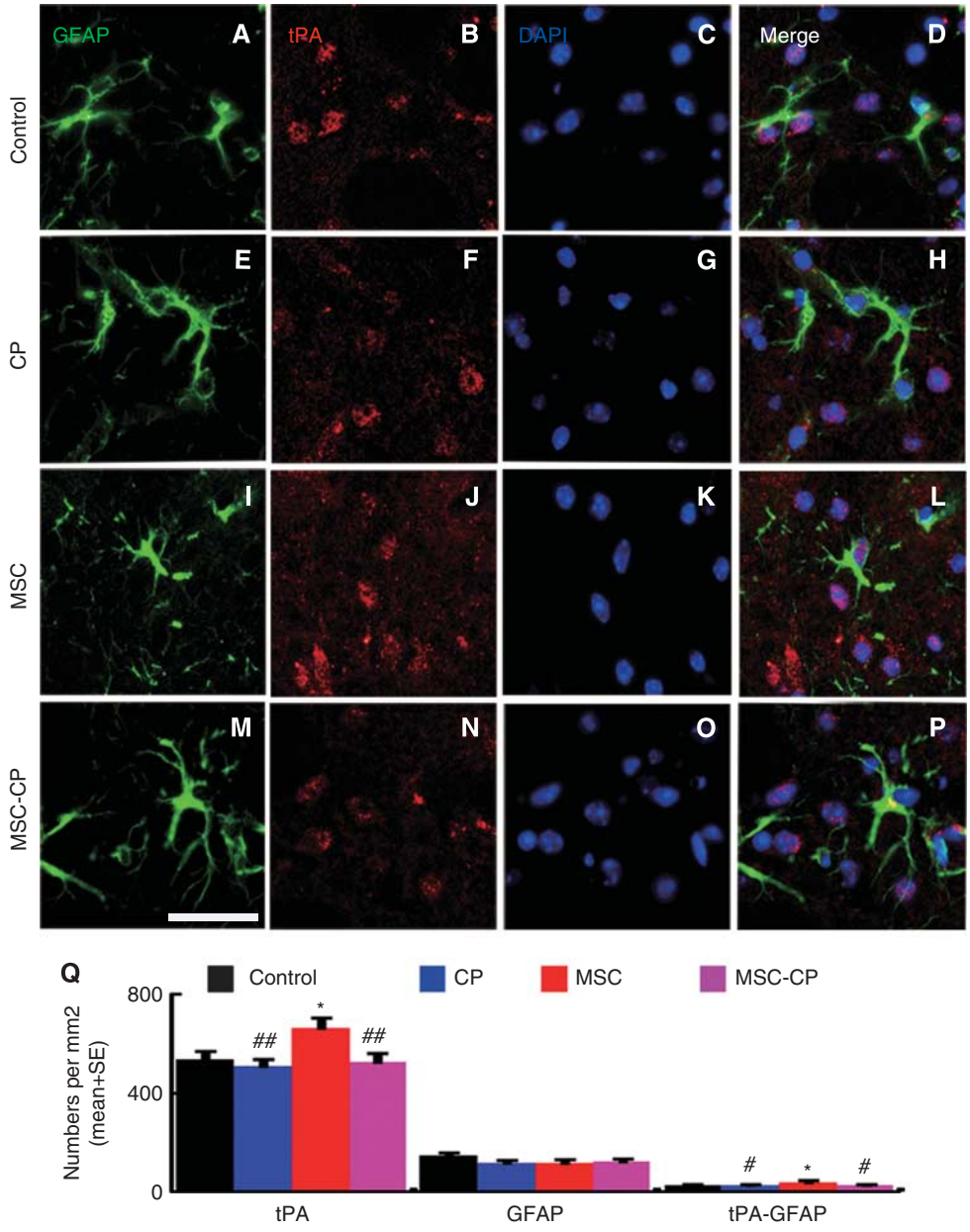

Figure 3. Double-staining immunohistochemistry of brain sections identifies cell types that express tissue plasminogen activator (tPA) in the ischemic boundary zone . Tissue plasminogen activator was co-localized with the astrocytic marker GFAP (**L**). Marrow stromal cell (MSC) treatment (**J**) significantly increased tPA expression in comparison with control (**B**), but cyclopamine (CP) completely reversed this effect (**F**). In the marrow stromal cells and cyclopamine (MSC-CP) group (**N**), tPA expression was same as with CP mono-treatment and control. Scale bars = 40 μm. Control: mice administered with 2-hydroxypropyl-β-cyclodextrin, $n=9$ (**A**–**D**); CP: mice administered with cyclopamine, $n=6$ (**E**–**H**); MSC: mice administered with bone MSCs, $n=9$ (**I**–**L**); MSC-CP: mice administered with bone MSCs and CP, $n=9$ (**M**–**P**). Quantification of immunostaining positive staining cells (**Q**). $^{*}P<0.05$ versus control; $^{\#}P<0.05$, $^{\#\#}P<0.01$ versus MSC.

the ratio of the synapse density between these 2 areas. The results showed that synapse density increased to 67% in the MSC group compared with 47% in control, 28% in CP, and 34% in MSC-CP ($P<0.05$, Figure 2J). Synaptophysin expression and synapse density were not significantly different among MSC-CP, CP, and control mice. These data indicated synaptic plasticity and synaptogenesis were increased after MSC treatment.

Bielschowsky silver is a marker for axons, and Luxol fast blue shows myelin in the white matter of the brain. A brain coronal section shows Bielschowsky sliver and Luxol fast blue-positive myelinated axons (Figure 2K). Areas with Bielschowsky sliver and Luxol fast blue expression-positive axons in the IBZ were significantly increased in MSC treated mice compared with mice in control, CP and MSC-CP groups ($P<0.01$) at 14 days after stroke, respectively (Figures 2M–P).

Marrow Stromal Cell Treatment Increases Tissue Plasminogen Activator and Sonic Hedgehog Levels in the Ischemic Boundary Zone

To clarify the relationship of the expressions of tPA in astrocytes and neurons, double immunostaining of tPA/GFAP (Figures 3A–Q) and tPA/NeuN (Figures 4A–Q) were performed. Tissue plasminogen activator-positive cells were $GFAP^+$ and $NeuN^+$. The numbers of $tPA^+/GFAP^+$ cells were 27, 27, 40, and 29 per mm^2 in control, CP, MSC, and MSC-CP groups, respectively, and the number of tPA^+/

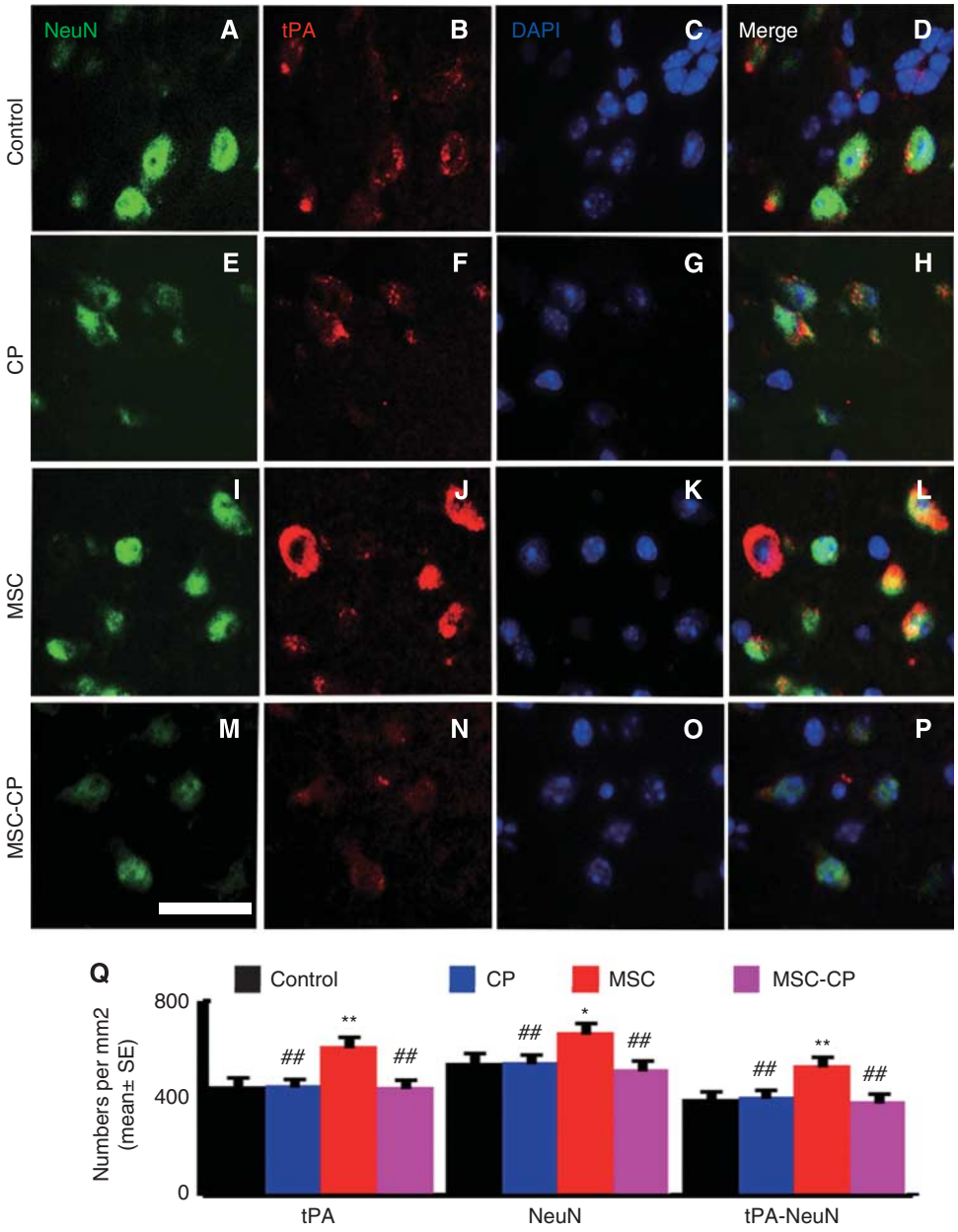

Figure 4. Double-staining immunohistochemistry of brain sections identifies cell types that express tissue plasminogen activator (tPA) in the ischemic boundary zone. Tissue plasminogen activator (tPA) was co-localized with neuron specific protein NeuN (**D**, **H**, **L**, **P**). Marrow stromal cell treatment (**J**) significantly increased tPA expression in comparison with the control and treatment groups (**B**, **F**, **N**). Tissue plasminogen activator expression was no differenceamong control, cyclopamine (CP), and marrow stromal cells and cyclopamine groups. Scale bars = 40 μm. Control: mice administered with 2-hydroxypropyl-β-cyclodextrin, $n=9$ (**A**–**D**); CP: mice administered with CP, $n=6$ (**E**–**H**); MSC: mice administered with bone MSCs, $n=9$ (**I**–**L**); MSC-CP: mice administered with bone MSCs and CP, $n=9$ (**M**–**P**). Quantification of immunostaining positive staining cells (**Q**). $^*P<0.05$, $^{**}P<0.01$ * versus control; $^{\#}P<0.05$, $^{\#\#}P<0.01$ versus marrow stromal cell.

NeuN$^+$ cells were 395, 406, 533, and 388 per mm^2, respectively. Consistent with our previous data, MSC treatment significantly increased tPA expression both in astrocytes and neurons, but CP reversed this effect completely. After administration of MSCs and CP together, the tPA expression did not increase, and was the same as with CP mono-treatment and control. These data suggest that CP blocks the effect of MSCs in promoting tPA expression.

To test whether MSCs activate the Shh pathway, Shh immunostaining was performed. Shh$^+$ cells were present in the IBZ at 14 days after MCAo in all mice. Sonic hedgehog expression was significanly increased in MSC-treated mice (Figures 5J and 6J, $P<0.05$), compared with control mice (Figures 5B and 6B). Double immunostaining of Shh/GFAP (Figures 5A–Q) and Shh/NeuN (Figures 6A–Q), showed that Shh$^+$ cells co-localized with GFAP$^+$ astrocytes and NeuN$^+$ neurons. The treatment of MSC-CP or CP did not change the Shh expression compared with control. Taken together with the above tPA immunostaining data, our data indicate that Shh increases tPA expression, which can be blocked by cyclopamine.

MSCs Promote Neurite Outgrowth via the Shh Pathway

The *in vivo* data suggest that activation of the Shh pathway by MSCs promoted neurite remodeling and CP reversed this effect. We also performed *in vitro* studies to confirm and further evaluate these results. A primary culture cortical neuronal system was employed to test whether MSCs increase neurite outgrowth. After normal culture or 2 hours OGD culture, primary cortical neurons

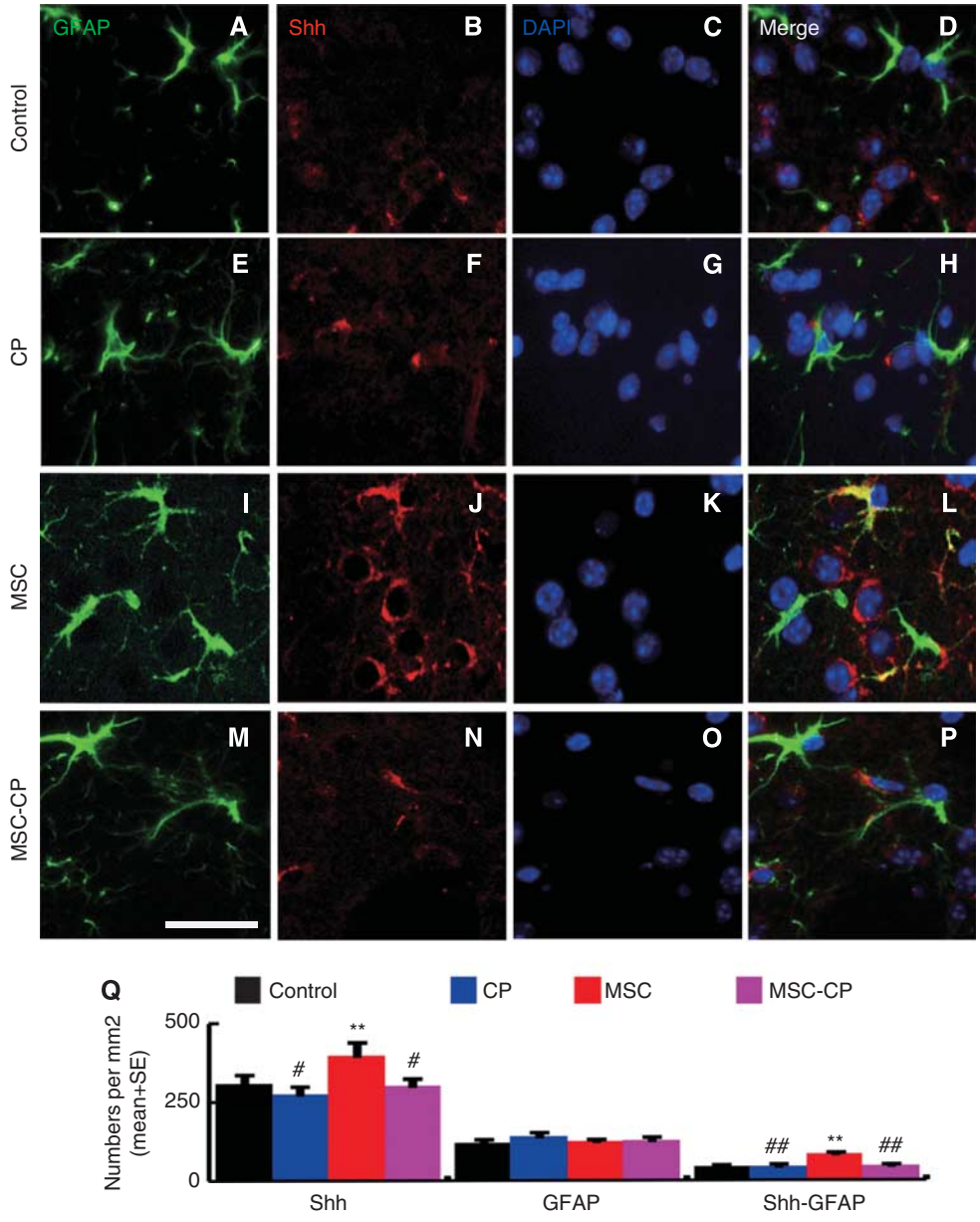

Figure 5. Double-staining immunohistochemistry of brain sections shows that sonic hedgehog (Shh) is expressed in astrocytes in the ischemic boundary zone. Sonic hedgehog was co-localized with the astrocytic marker GFAP (**L**). Significantly increased Shh expression was observed only in the marrow stromal cell (MSC) group but not in the control, cyclopamine (CP) and marrow stromal cells and cyclopamine (MSC-CP) groups (**B**, **F**, **J**, **N**). Scale bars = 40 μm. Control: mice administered with 2-hydroxypropyl-β-cyclodextrin, $n=9$ (**A**–**D**); CP: mice administered with CP, $n=6$ (**E**–**H**); MSC: mice administered with bone MSCs, $n=9$ (**I**–**L**); MSC-CP: mice administered with bone MSCs and CP, $n=9$ (**M**–**P**). Quantification of immunostaining positive staining cells (**Q**). $^{**}P<0.01$ versus control; $^{\#}P<0.05$, $^{\#\#}P<0.01$ versus MSC.

were treated with Shh, or CP, or co-cultured with MSCs and normal astrocytes, or co-cultured with MSCs and OGD astrocytes for 3 days. Figures 7A–J shows the typical morphology of cultured neurons with different treatments. Sonic hedgehog treatment significantly increased the neurite branch number and total neurite length, compared with normal or OGD cultured neurons, and similar results were observed in normal or OGD cultured neurons co-cultured with MSCs and normal or OGD astrocytes, respectively (Figures 7K and L). In contrast, CP treatment decreased neurite number and total neurite length compared with normal and OGD cultured neurons. Figure 7M shows that MSC and normal or OGD astrocyte co-culture significantly increased Shh secretion in the medium of normal and OGD cultured neurons ($P<0.01$). Cyclopamine treatment did not significantly affect Shh concentration. Marrow stromal cell and astrocyte co-culture with neurons increased both the Shh concentration in the medium and the neurite branches. These data suggest that MSCs increase neurite outgrowth via the Shh pathway.

DISCUSSION

In the present study, we have demonstrated that MSCs evoke significant improvement in functional neurologic recovery after focal brain ischemia. Using immunostaining, electron microscopy, and histochemistry staining, respectively, we also observed that MSC treatment significantly increases synaptophysin level,

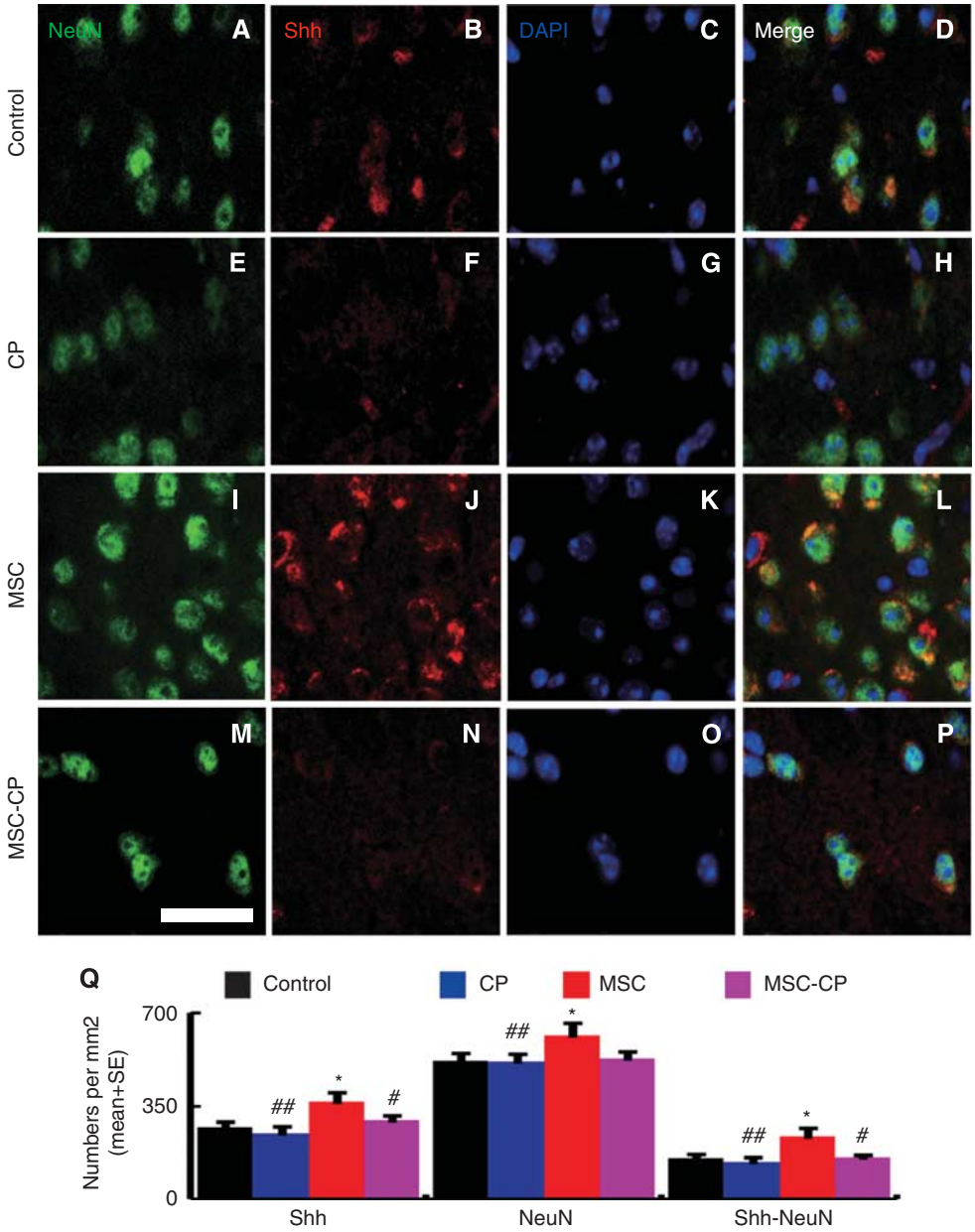

Figure 6. Double-staining immunohistochemistry of brain sections shows that sonic hedgehog (Shh) is expressed in neurons; Shh was co-localized with neuron-specific protein NeuN (**D**, **H**, **L**, **P**). After treated with marrow stromal cell (MSC) (**J**), Shh expression in the ischemic boundary zone was significantly increased compared with control (**B**). Cyclopamine (CP) mono-treatment or CP combined with MSC both abolished this effect (**F**, **N**). Scale bars = 40 μm. Control: mice administered with 2-hydroxypropyl-β-cyclodextrin, $n=9$ (**A**–**D**); CP: mice administered with CP, $n=6$, (**E**–**H**); MSC: mice administered with bone MSCs, $n=9$ (**I**–**L**); MSC-CP: mice administered with bone MSCs and CP, $n=9$ (**M**–**P**). Quantification of immunostaining positive staining cells (**Q**). $^{*}P<0.05$ versus control; $^{\#}P<0.05$, $^{\#\#}P<0.01$ versus MSC.

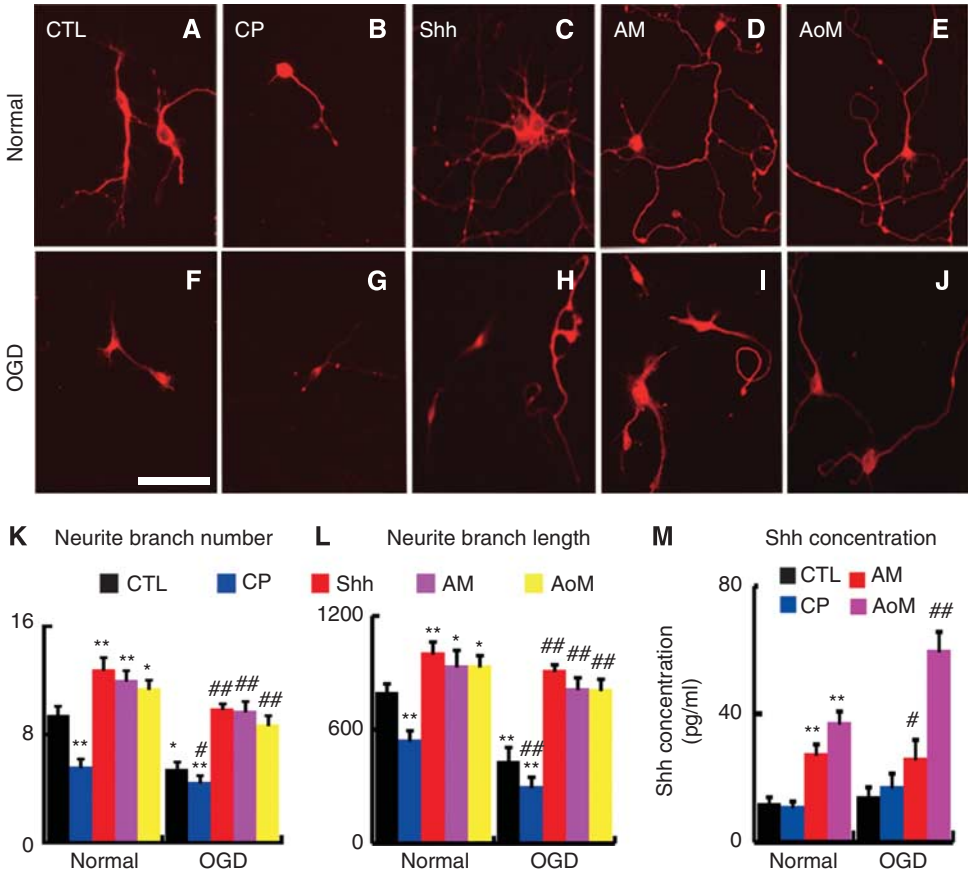

Figure 7. Compared to normal or oxygen-glucose deprived (OGD) cultured neurons (**A**, **F**), sonic hedgehog (Shh) treatment significantly increased the neurite branch number and total neurite length (**C**, **H**), and similar results were observed in normal or OGD cultured neurons co-cultured with marrow stromal cells (MSCs) and normal or OGD astrocytes (**D**, **E**, **I**, **J** and **K**, **L**, respectively). Cyclopamine treatment decreased neurite number and total neurite length (**B**, **G**). Marrow stromal cell and astrocyte co-culture significantly increased Shh secretion in the medium of normal and OGD cultured neurons (**M**, $P<0.01$). Cyclopamine did not affect Shh concentration. Scale bars = 50 μm. CTL: control neurons; CP: treated neurons with CP; Shh: treated neurons with Shh; AM: co-cultured neurons with astrocytes and MSCs; AoM: co-cultured neurons with MSCs and OGD astrocytes; $^{*}P<0.05$,$^{**}P<0.01$ versus normal control neurons, $^{\#}P<0.05$, $^{\#\#}P<0.01$ versus OGD neurons.

synapse density, and axonal density. Synapse reorganization and axon remodeling are likely the most important steps driving neurologic function recovery. These results are consistent with previous reports.[4,5,18] In addition, we demonstrate, for the first time, that the beneficial effects of MSC treatment can be blocked by the Shh inhibitor, cyclopamine. The *in vivo* data also support an interaction between the Shh signaling pathway and tPA during MSC promotion of brain plasticity post stroke. Marrow stromal cell-treated mice had a more robust increase in tPA expression and Shh expression in the IBZ compared with control animals, which were counteracted by combined treatment with cyclopamine. Application of cyclopamine alone had no effect on neurologic recovery, and had similar outcomes as cyclopamine in combination with MSCs. In addition, combined MSC treatment with cyclopamine reduced neurite outgrowth and functional benefit compared with MSC-treated animals. Consistent with the above results, *in vitro* data show that Shh treatment of primary neurons showed significant increase of neurite outgrowth. In addition, co-culture of primary neurons with MSCs and normal or OGD astrocytes significantly increased neurite outgrowth and Shh concentration when measured by ELISA assay. However, when cyclopamine, a known inhibitor of Shh pathway, was used to treat primary neurons, it was observed that neurite outgrowth significantly decreased. Cyclopamine directly inhibits Smoothened, the downstream protein of Shh, and the Shh concentration in the media of cyclopamine-treated neurons was not significantly decreased.

Marrow stromal cell-based therapy has shown remarkable ability to improve neurologic function when administered after stroke onset. Marrow stromal cells promote axonal sprouting,[19] synaptic reorganization,[4] oligodendrogenesis,[1] angiogenesis,[20] and secretion of bioactive factors after focal brain ischemia.[20,21] Marrow stromal cells significantly improve functional recovery in wild-type mice but show no beneficial effect in the tPA$^{-/-}$ mice.[4] In the IBZ, MSCs significantly increase plasmin activity.[5] *In vitro*, tPA in the cultured medium from MSCs contributes to neurite outgrowth, and blockage of tPA can attenuate this effect.[6] Tissue plasminogen activator is crucial for axonal regeneration,[22,23] and is a key mediator during MSC-induced neurite outgrowth.[4,5,22,24] As a major serine protease in the central nervous system, tPA can be produced by neurons, astrocytes, microglia, and endothelial cells.[5,25,26] Our data demonstrate that after MSC treatment, tPA is co-localized with neurons and astrocytes, and its expression is significantly increased and accompanies partial recovery of neurologic function. Tissue plasminogen activator can interact with parenchymal cells through proteolytic plasminogen/plasmin function to cleave the neurotrophin precursors into the active trophic factors,[27,28] or stimulate nitric oxide synthase (NOS) to increase nitric oxide (NO) and which subsequently increases cyclic guanosine monophosphate (cGMP).[29] Tissue plasminogen activator also interacts with other effectors such as low-density lipoprotein receptor-related protein and platelet-derived growth factor.[30,31] These interactions likely promote tPA-mediated

neurorestorative processes after stroke. In the present study, we show that blocking Shh with cyclopamine significantly reduces the MSC-evoked increase in tPA (Figure 3). *In vitro* studies also demonstrated that the Shh pathway mediates neurite outgrowth via tPA.[6,7] Thus, our data indicate that MSCs mediate the increase of tPA via the Shh pathway and thereby promote cerebral plasticity and neurologic function.

Sonic hedgehog promotes neurogenesis in the hippocampal subgranular zone (SGZ) and the subventricular zone (SVZ).[32,33] After brain injury, the Shh-signaling pathway is activated and induces regenerative roles in reactive gliosis.[34] Marrow stromal cells enhance functional recovery post stroke, which may be related to the Shh-signaling pathway.[35] We propose a hypothesis that the Shh-signaling pathway promotes the MSC-mediated activation of tPA in parenchymal cells. We therefore employed mice subjected to MCAo and treated with the selective Shh-pathway inhibitor, cyclopamine, or MSCs as a monotherapy, or combination of cyclopamine and MSCs, to dissect the relationship between Shh and tPA. In agreement with our hypothesis, the increase of tPA caused by MSCs can be reversed by cyclopamine during combined application. Comparison of cyclopamine mono-treatment with combination treatment with cyclopamine and MSCs of MCAo mice, showed no differences on tPA expression.

By using cyclopamine to block the Shh pathway *in vivo*, we support the hypothesis that MSC treatment of stroke stimulates Shh and thereby increases tPA expression. Double staining, further reveals that astrocytes and neurons express tPA. We, however, do not exclude the possibility that other parenchymal cells express tPA post MSC treatment of stroke. Our previous *in vitro* study also demonstrated that MSCs increase Shh, which subsequently increases tPA expression and decreases PAI-1 expression in OGD astrocytes.[6,7] Taken together with our current data, we propose that the parenchymal cell increase of Shh resulting from MSC treatment increases tPA expression, which promotes axonal remodeling and neurite outgrowth. The question arises, what is the source of Shh? Do MSCs generate Shh and/or do they stimulate expression of Shh in the parenchymal cells? Only a very small portion (approximately 1%) of injected MSCs can be detected in brain parenchyma at 14 days after transplantation[36] and the very few and scattered MSC are unlikely the direct source of Shh. Moreover, Shh expression at the protein level and mRNA level by MSCs is very low and essentially below detection limits.[6,37] Recently, we have demonstrated that MSCs release exosomes containing microRNAs, which may mediate gene expression in parenchymal cells.[38] This pathway for MSC-mediated stimulation of Shh in parenchymal cells warrants further investigation.

After more than a decade of investigating mechanisms underlying the therapeutic effects of MSC-based therapy, we have moved from the early assumption that MSCs are stem like, and replace dead neural tissue to the assumption that MSCs stimulate the injured brain and evoke restorative events, which remodel the central nervous system and lead to improvement of neurological outcome.[4,20,39,40] The novel insights of the present study include that MSCs, exogenously administered cells, may act as 'catalysts', which activate parenchymal cells, most likely the astrocytes, to stimulate endogenous restorative mechanism. We also provide the molecular basis for the intercellular communication between exogenous cells and parenchymal cells that Shh mediates the enhancement of tPA activity. This study provides a new framework to understand the basis of restorative MSC-based therapy for stroke. More effective endogenous stimulation of Shh in brain parenchymal cells may further enhance restorative therapy for stroke and possibly other neurologic diseases.

Collectively, these *in vivo* and *in vitro* data strongly support a role of MSCs stimulating Shh in parenchymal cells to promote brain plasticity and behavioral recovery from stroke.

DISCLOSURE/CONFLICT OF INTEREST

The authors declare no conflict of interest.

ACKNOWLEDGEMENTS

We thank Drs Mei Lu and Talan Zhang for statistical analysis assistance; Thomas G Christopherson for assistance in Electron Microscopy; Cynthia Roberts, Qing-e Lu, and Sutapa Santra for technical assistance on histology.

REFERENCES

1 Li Y, Chen J, Zhang CL, Wang L, Lu D, Katakowski M *et al.* Gliosis and brain remodeling after treatment of stroke in rats with marrow stromal cells. *Glia* 2005; **49**: 407–417.
2 Li Y, McIntosh K, Chen J, Zhang C, Gao Q, Borneman J *et al.* Allogeneic bone marrow stromal cells promote glial-axonal remodeling without immunologic sensitization after stroke in rats. *Exp Neurol* 2006; **198**: 313–325.
3 Liu Z, Li Y, Zhang ZG, Cui X, Cui Y, Lu M *et al.* Bone marrow stromal cells enhance inter- and intracortical axonal connections after ischemic stroke in adult rats. *J Cereb Blood Flow Metab* 2010; **30**: 1288–1295.
4 Shen LH, Xin H, Li Y, Zhang RL, Cui Y, Zhang L *et al.* Endogenous tissue plasminogen activator mediates bone marrow stromal cell-induced neurite remodeling after stroke in mice. *Stroke* 2011; **42**: 459–464.
5 Xin H, Li Y, Shen LH, Liu X, Wang X, Zhang J *et al.* Increasing tPA activity in astrocytes induced by multipotent mesenchymal stromal cells facilitate neurite outgrowth after stroke in the mouse. *PLoS One* 2010; **5**: e9027.
6 Xin H, Li Y, Shen LH, Liu X, Hozeska-Solgot A, Zhang RL *et al.* Multipotent mesenchymal stromal cells increase tPA expression and concomitantly decrease PAI-1 expression in astrocytes through the sonic hedgehog signaling pathway after stroke (in vitro study). *J Cereb Blood Flow Metab* 2011; **31**: 2181–2188.
7 Teng H, Chopp M, Hozeska-Solgot A, Shen L, Lu M, Tang C *et al.* Tissue plasminogen activator and plasminogen activator inhibitor 1 contribute to sonic hedgehog-induced in vitro cerebral angiogenesis. *PLoS One* 2012; **7**: e33444.
8 Marti E, Bovolenta P. Sonic hedgehog in CNS development: one signal, multiple outputs. *Trends Neurosci* 2002; **25**: 89–96.
9 Stecca B, Mas C, Clement V, Zbinden M, Correa R, Piguet V *et al.* Melanomas require HEDGEHOG-GLI signaling regulated by interactions between GLI1 and the RAS-MEK/AKT pathways. *Proc Natl Acad Sci USA* 2007; **104**: 5895–5900.
10 Johnson RW, Nguyen MP, Padalecki SS, Grubbs BG, Merkel AR, Oyajobi BO *et al.* TGF-beta promotion of Gli2-induced expression of parathyroid hormone-related protein, an important osteolytic factor in bone metastasis, is independent of canonical Hedgehog signaling. *Cancer Res* 2011; **71**: 822–831.
11 Gould S, Scott RC. 2-Hydroxypropyl-beta-cyclodextrin (HP-beta-CD): a toxicology review. *Food Chem Toxicol* 2005; **43**: 1451–1459.
12 Chen J, Zhang C, Jiang H, Li Y, Zhang L, Robin A *et al.* Atorvastatin induction of VEGF and BDNF promotes brain plasticity after stroke in mice. *J Cereb Blood Flow Metab* 2005; **25**: 281–290.
13 Zhang Y, Da RR, Hilgenberg LG, Tourtellotte WW, Sobel RA, Smith MA *et al.* Clonal expansion of IgA-positive plasma cells and axon-reactive antibodies in MS lesions. *J Neuroimmunol* 2005; **167**: 120–130.
14 Buller B, Liu X, Wang X, Zhang RL, Zhang L, Hozeska-Solgot A *et al.* MicroRNA-21 protects neurons from ischemic death. *FEBS J* 2010; **277**: 4299–4307.
15 Lu M, Chen J, Lu D, Yi L, Mahmood A, Chopp M. Global test statistics for treatment effect of stroke and traumatic brain injury in rats with administration of bone marrow stromal cells. *J Neurosci Methods* 2003; **128**: 183–190.
16 Hallett M. Plasticity of the human motor cortex and recovery from stroke. *Brain Res Brain Res Rev* 2001; **36**: 169–174.
17 Calhoun ME, Jucker M, Martin LJ, Thinakaran G, Price DL, Mouton PR. Comparative evaluation of synaptophysin-based methods for quantification of synapses. *J Neurocytol* 1996; **25**: 821–828.
18 Shen LH, Li Y, Chen J, Cui Y, Zhang C, Kapke A *et al.* One-year follow-up after bone marrow stromal cell treatment in middle-aged female rats with stroke. *Stroke* 2007; **38**: 2150–2156.
19 Liu Z, Li Y, Qu R, Shen L, Gao Q, Zhang X *et al.* Axonal sprouting into the denervated spinal cord and synaptic and postsynaptic protein expression in the spinal cord after transplantation of bone marrow stromal cell in stroke rats. *Brain Res* 2007; **1149**: 172–180.
20 Chen J, Zhang ZG, Li Y, Wang L, Xu YX, Gautam SC *et al.* Intravenous administration of human bone marrow stromal cells induces angiogenesis in the ischemic boundary zone after stroke in rats. *Circ Res* 2003; **92**: 692–699.
21 Shen LH, Li Y, Chopp M. Astrocytic endogenous glial cell derived neurotrophic factor production is enhanced by bone marrow stromal cell transplantation in the ischemic boundary zone after stroke in adult rats. *Glia* 2010; **58**: 1074–1081.

22 Liu Z, Li Y, Zhang L, Xin H, Cui Y, Hanson LR *et al*. Subacute intranasal administration of tissue plasminogen activator increases functional recovery and axonal remodeling after stroke in rats. *Neurobiol Dis* 2012; **45**: 804–809.
23 Akassoglou K, Kombrinck KW, Degen JL, Strickland S. Tissue plasminogen activator-mediated fibrinolysis protects against axonal degeneration and demyelination after sciatic nerve injury. *J Cell Biol* 2000; **149**: 1157–1166.
24 Zhang L, Zhang ZG, Ding GL, Jiang Q, Liu X, Meng H *et al*. Multitargeted effects of statin-enhanced thrombolytic therapy for stroke with recombinant human tissue-type plasminogen activator in the rat. *Circulation* 2005; **112**: 3486–3494.
25 Tsirka SE, Rogove AD, Bugge TH, Degen JL, Strickland S. An extracellular proteolytic cascade promotes neuronal degeneration in the mouse hippocampus. *J Neurosci* 1997; **17**: 543–552.
26 Kim JA, Tran ND, Li Z, Yang F, Zhou W, Fisher MJ. Brain endothelial hemostasis regulation by pericytes. *J Cereb Blood Flow Metab* 2006; **26**: 209–217.
27 Barnes P, Thomas KL. Proteolysis of proBDNF is a key regulator in the formation of memory. *PLoS One* 2008; **3**: e3248.
28 Pang PT, Teng HK, Zaitsev E, Woo NT, Sakata K, Zhen S *et al*. Cleavage of proBDNF by tPA/plasmin is essential for long-term hippocampal plasticity. *Science* 2004; **306**: 487–491.
29 Zhang N, Beuve A, Townes-Anderson E. The nitric oxide-cGMP signaling pathway differentially regulates presynaptic structural plasticity in cone and rod cells. *J Neurosci* 2005; **25**: 2761–2770.
30 An J, Zhang C, Polavarapu R, Zhang X, Yepes M. Tissue-type plasminogen activator and the low-density lipoprotein receptor-related protein induce Akt phosphorylation in the ischemic brain. *Blood* 2008; **112**: 2787–2794.
31 Su EJ, Fredriksson L, Geyer M, Folestad E, Cale J, Andrae J *et al*. Activation of PDGF-CC by tissue plasminogen activator impairs blood-brain barrier integrity during ischemic stroke. *Nat Med* 2008; **14**: 731–737.
32 Jiao J, Chen DF. Induction of neurogenesis in nonconventional neurogenic regions of the adult central nervous system by niche astrocyte-produced signals. *Stem Cells* 2008; **26**: 1221–1230.
33 Fredriksson L, Li H, Fieber C, Li X, Eriksson U. Tissue plasminogen activator is a potent activator of PDGF-CC. *EMBO J* 2004; **23**: 3793–3802.
34 Amankulor NM, Hambardzumyan D, Pyonteck SM, Becher OJ, Joyce JA, Holland EC. Sonic hedgehog pathway activation is induced by acute brain injury and regulated by injury-related inflammation. *J Neurosci* 2009; **29**: 10299–10308.
35 Zhang J, Li Y, Zhang ZG, Lu M, Borneman J, Buller B *et al*. Bone marrow stromal cells increase oligodendrogenesis after stroke. *J Cereb Blood Flow Metab* 2009; **29**: 1166–1174.
36 Chen J, Li Y, Wang L, Zhang Z, Lu D, Lu M *et al*. Therapeutic benefit of intravenous administration of bone marrow stromal cells after cerebral ischemia in rats. *Stroke* 2001; **32**: 1005–1011.
37 Kramer BC, Woodbury D, Black IB. Adult rat bone marrow stromal cells express genes associated with dopamine neurons. *Biochem Biophys Res Commun* 2006; **343**: 1045–1052.
38 Xin H, Li Y, Buller B, Katakowski M, Zhang Y, Wang X *et al*. Exosome-mediated transfer of miR-133b from multipotent mesenchymal stromal cells to neural cells contributes to neurite outgrowth. *Stem Cells* 2012; **30**: 1556–1564.
39 Lu D, Mahmood A, Wang L, Li Y, Lu M, Chopp M. Adult bone marrow stromal cells administered intravenously to rats after traumatic brain injury migrate into brain and improve neurological outcome. *Neuroreport* 2001; **12**: 559–563.
40 Zhang J, Li Y, Chen J, Cui Y, Lu M, Elias SB *et al*. Human bone marrow stromal cell treatment improves neurological functional recovery in EAE mice. *Exp Neurol* 2005; **195**: 16–26.